JOURNAL OF GUIDANCE, CONTROL, AND DYNAMICS
Vol. 27, No. 2, March–April 2004

Nonlinear Control of Librational Motion of Tethered Satellites in Elliptic Orbits

Hirohisa Kojima,* Masatake Iwasaki,† and Hironori A. Fujii‡
Tokyo Metropolitan Institute of Technology, Tokyo 191-0065, Japan
and
Chris Blanksby§ and Pavel Trivailo¶
RMIT University, Melbourne, Victoria 3001, Australia

A method to control the librational motion of a tethered satellite system in an elliptic orbit is presented. To simplify the analysis, gravity is treated as the only external force affecting the tethered satellite system, only in-plane motion is considered, and the flexibility and mass of tethers are neglected. The tethered satellite system treated in this paper consists of two subsatellites and a mother satellite, such as the space shuttle, connected together in series via massless tethers. This type of tethered satellite system has very important applications in Earth observation, space observation, communications, and satellite constellations. The librational motion of the tethered satellite system in an elliptic orbit is known to be chaotic and can be stabilized to undergo periodic motion by the delayed feedback control method. The periodic motion of a tethered satellite in a circular orbit is employed as the reference trajectory for tracking by the actual tethered satellite, which is in an elliptic orbit. The decoupling and model tracking control methods, based on differential geometric control theory are combined with the delayed feedback control method in a new approach to controlling the librational motion of the tethered satellite system in elliptic orbits. The results of numerical simulations show that the proposed control scheme has good performance in controlling the librational motion of a tethered satellite system in an elliptic orbit.

Introduction

THIS paper introduces two new developments in the field of nonlinear control of tethered satellite systems. The first of these is the application of the existing delayed feedback nonlinear control technique, developed by Ott et al.[1] and Pyragas,[2] to control the librations of a three-mass space tether system comprising a mother satellite, such as the space shuttle, and two smaller subsatellites, in elliptic orbits. The three-mass space tether system has some very important applications in space science and communications, such as the observation of meteors and aurora from more than two directions simultaneously and constellation flight for conducting radio telescope in space. The second innovation introduced in this paper is a new control method combining the delayed feedback method with the model-following, decoupling-control method based on differential geometric control theory.[3] The present method is also applied to the problem of controlling librations in a three-mass tethered satellite system in an elliptical orbit. Simulation results produced for both methods are included, which indicate that the new method has significant advantages. Both methods are able to control the three-mass tethered satellite system, and this in itself has important implications for the future development of such systems.

Received 23 December 2002; revision received 23 June 2003; accepted for publication 9 July 2003.

*Lecturer, Department of Aerospace Engineering, 6-6 Asahigaoka, Hino; kojima@krasklab6.tmit.ac.jp. Member AIAA.

†Graduate Student, Department of Aerospace Engineering, 6-6 Asahigaoka, Hino; currently Expert, Research and Development Headquarters, NTT DATA Corporation, Toyosu Center Building 3-3, Toyosu 3-chome, Koto-ku, 135-6033.

‡Professor, Department of Aerospace Engineering, 6-6 Asahigaoka, Hino; Associate Fellow AIAA.

§Senior Research Fellow, School of Aerospace, Mechanical and Manufacturing Engineering, G.P.O. Box 2476V.

¶Associate Professor, Director, School of Aerospace, Mechanical and Manufacturing Engineering, G.P.O. Box 2476V.

Tethered satellite systems are expected to be an effective part of infrastructure in space for constructing large space structures, observing the atmosphere of the Earth, creating artificial gravitational force, and generating electric power. The three-mass tethered satellite system is a development of the conventional dumbbell (two-mass) tethered satellite system, and introduces an extra degree of freedom, thereby offering significant advantages in the preceding applications and enabling several new applications. The three-mass tethered satellite system also introduces additional control variables and complicates the dynamics of the system beyond those of the dumbbell system.

Because of the complex dynamics, controlling tether motion by traditional linear control theory is difficult, and thus the investigation of new methods for analyzing and controlling the motion of the tethered subsatellite system is important. For this reason several researchers have been investigating the motion of the tethered satellite system with respect to various aspects.[4–12]

The librational or attitude motion of the tethered satellite system is one of its nonlinear characteristics. The librational motion of the tethered satellite system behaves chaotically as a result of the gravity gradient when the orbit is eccentric. The nature of the chaotic motion changes with increasing eccentricity. Poincare maps and Lyapunov exponents are useful tools for analyzing the nonlinear dynamics and have been used to analyze the gravity-gradient satellite.[5,6] These techniques have also been applied to analysis of the librational motion of the tethered satellite system.[7,8]

The librational motion of the tethered satellite system must be controlled when the system is used for scientific missions. Chaos observed in the motion of the tethered satellite system can be controlled by nonlinear control methods such as delayed feedback control. Delayed feedback control adds a periodic control input to the system in order to stabilize the chaotic motion and has been studied to control the gravity-gradient satellite.[9,10] This method has been also studied to regulate librational motion of the tethered satellite in elliptic orbits into periodic solutions.[11,12]

The preceding research, however, has treated only the tether dumbbell model with two satellites. An example of such a system is a tether satellite operated from the space shuttle. To extend the capability of the tethered satellite system, tethered satellite systems that include more than two subsatellites should be investigated.

In several cases the two-mass tether system will be required to operate in an elliptical orbit. Even if intended for a circular orbit, the motion of the tethered satellite system depends on the initial conditions by which the system is launched into orbit, and the system can rarely be launched into a circular orbit because of errors such as misfires. Thus, it is very important to consider the control of librations for the three-mass tether system in elliptical orbits.

In the present paper, to simplify the analysis, gravity is treated as the only external force affecting the tethered satellite system, and only in-plane motion is considered. In addition, the mass and flexibility of tethers are neglected. Even under these assumptions, the librational motion of this system behaves chaotically. The effectiveness of the delayed feedback control method has previously been studied to stabilize this chaotic librational motion of a two-mass tether satellite to periodic motion,[11,12] but has not been studied for a three-mass tethered satellite system. The delayed feedback control is a good approach to controlling the system because real-time feedback control cannot be realized in practice. Thus, we first consider the delayed feedback control method for controlling the librational motion of a three-mass tether system. After that the decoupling method based on differential geometric theory is studied to control each tether angle independently, where the equilibrium angles of the tethered satellite in a circular orbit are employed as the reference angles for tracking by the tethered satellite in an elliptic orbit. If each tether angle is controlled independently, scientific missions such as the observation of meteors or aurora can be conducted from two directions simultaneously, and constellation flight in space can be achieved. Finally, the proposed method combining the delayed feedback control with model-following and decoupling-control method based on differential geometric control theory is employed to control the librational motion of the tethered satellite system in an elliptic orbit, where the reference motion is a periodic motion that is adequately stabilized by the delayed feedback control. The results of numerical simulations indicate that the control scheme, integrating three different techniques, has good performance in controlling the librational motion of the tethered satellite system in an elliptic orbit because the settling time to a periodic solution by the proposed method is much shorter than that of the delayed feedback control, and the control forces after the librational motion is stabilized to a periodic motion become sufficiently small even if the system is in an elliptic oribt.

Model Description

System Model

To investigate the effect of the gravity on the motion of the tethered subsatellite system, the elasticity of the tether and the aerodynamic drag force affecting the system are assumed to be negligible, and only the station-keeping phase and in-plane motions are treated in the present study. The center of mass of the system is unconstrained. However, it is assumed that the center of mass of the system maintains its elliptic orbit for all of the cases considered in the present paper. The motion of the tethered satellite system is classified into two types: librational motion and circular motion. The tethered subsatellite swings like a pendulum in the case of librational motion and rotates around the mother satellite in the case of circular motion.

The schematic model of the tethered subsatellite system treated in the present paper is illustrated in Fig. 1. This system consists of a mother satellite such as the space shuttle, two subsatellites, and two tethers. The mother satellite and two subsatellites are labeled 0, 1, and 2, respectively, and are assumed to be particles with masses m_0, m_1, and m_2, respectively. Tethers 1 and 2 are assumed to be rigid bodies without mass or inertia. Subsatellite 1 is connected to the mother satellite by tether 1 with length l_1 and connected to subsatellite 2 by tether 2 with length l_2. Thruster jets are assumed to be installed on subsatellites 1 and 2, and the direction of each thruster jet is assumed to be perpendicular to tethers 1 and 2, respectively. The vectors $\boldsymbol{F}_1$ and $\boldsymbol{F}_2$ denote the vectors of the thrusts on subsatellites 1 and 2, respectively, and the parameters F_1 and F_2 denote the magnitude of the thrusts on subsatellites 1 and 2, respectively. The vectors $\boldsymbol{R}_c$, $\boldsymbol{R}_0$, $\boldsymbol{R}_1$, and $\boldsymbol{R}_2$ denote position vectors of the center of mass of the system, the mother satellite, and subsatellites 1 and 2, respectively. The vector from the center of mass of the system to the mother satellite is denoted by $\boldsymbol{r}_0$. The vectors $\boldsymbol{i}$ and $\boldsymbol{j}$ are an orthogonal set of unit vectors with $\boldsymbol{i}$ corresponding to the direction from the center of the Earth to the center of mass of the system. The vectors $\boldsymbol{l}_1$ and $\boldsymbol{l}_2$ are the directions from the mother satellite to subsatellite 1 and from subsatellite 1 to subsatellite 2, respectively. The parameter η is the true anomaly of the center of mass of the system. The parameters θ_1 and θ_2 are the angles of tethers 1 and 2 relative to directions $\boldsymbol{i}$ and $\boldsymbol{l}_1$, respectively.

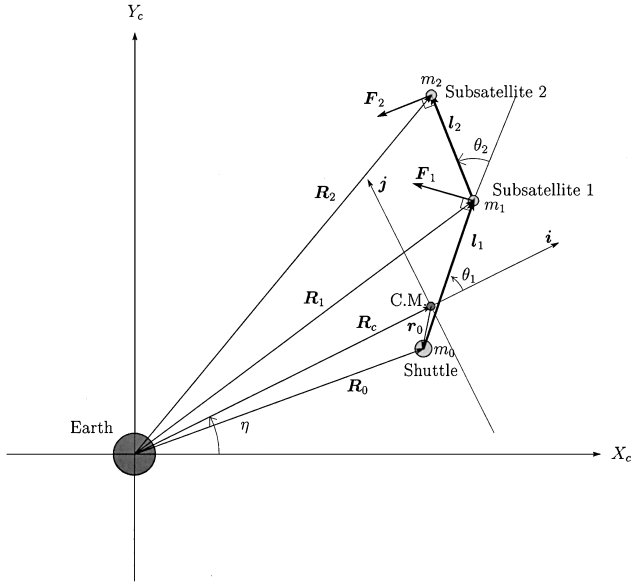

Fig. 1 Schematic model of the three-mass tethered satellite system.

Equations of Motion

The position vectors of the center of the mass of the system $\boldsymbol{R}_c$, the mother satellite $\boldsymbol{R}_0$, and the subsatellites $\boldsymbol{R}_1$ and $\boldsymbol{R}_2$ are, respectively,

$$\boldsymbol{R}_c = R_c \cdot \boldsymbol{i} \tag{1}$$

$$\boldsymbol{R}_0 = \boldsymbol{R}_c + \boldsymbol{r}_0 \tag{2}$$

$$\boldsymbol{R}_1 = \boldsymbol{R}_c + \boldsymbol{r}_0 + \boldsymbol{l}_1 \tag{3}$$

$$\boldsymbol{R}_2 = \boldsymbol{R}_c + \boldsymbol{r}_0 + \boldsymbol{l}_1 + \boldsymbol{l}_2 \tag{4}$$

where

$$\boldsymbol{r}_0 = -\frac{m_1 + m_2}{m_0 + m_1 + m_2} \cdot \boldsymbol{l}_1 - \frac{m_2}{m_0 + m_1 + m_2} \cdot \boldsymbol{l}_2 \tag{5}$$

$$\boldsymbol{l}_1 = l_1 \cos\theta_1 \cdot \boldsymbol{i} + l_1 \sin\theta_1 \cdot \boldsymbol{j} \tag{6}$$

$$\boldsymbol{l}_2 = l_2 \cos(\theta_1 + \theta_2) \cdot \boldsymbol{i} + l_2 \sin(\theta_1 + \theta_2) \cdot \boldsymbol{j} \tag{7}$$

Let us consider R_c, η, θ_1, and θ_2 as generalized coordinates and refer to each as q_1, q_2, q_3, and q_4, respectively. The generalized inertia force and the generalized active force of the system Q_k^* and Q_k, respectively, are

$$Q_k^* = -m_0\ddot{\boldsymbol{R}}_0 \cdot \boldsymbol{v}_{0k} - m_1\ddot{\boldsymbol{R}}_1 \cdot \boldsymbol{v}_{1k} - m_2\ddot{\boldsymbol{R}}_2 \cdot \boldsymbol{v}_{2k} \qquad (k = 1, 2, 3, 4) \tag{8}$$

$$Q_k = -\mu_e m_0\left(\boldsymbol{R}_0 \big/ R_0^3\right) \cdot \boldsymbol{v}_{0k} - \mu_e m_1\left(\boldsymbol{R}_1 \big/ R_1^3\right) \cdot \boldsymbol{v}_{1k} - \mu_e m_2\left(\boldsymbol{R}_2 \big/ R_2^3\right) \cdot \boldsymbol{v}_{2k} + \boldsymbol{F}_1 \cdot \boldsymbol{v}_{1k} + \boldsymbol{F}_2 \cdot \boldsymbol{v}_{2k} \qquad (k = 1, 2, 3, 4) \tag{9}$$

where μ_e is the gravity constant of the Earth and $\boldsymbol{v}_{jk}$ is the partial velocity vector of the ith body with respect to the generalized

speed $\dot{q}_k$. The equations of motion are obtained by employing Kane's equation[13]

$$Q_k + Q_k^* = 0 \qquad (k = 1, 2, 3, 4) \tag{10}$$

An implementation by Mathematica (Wolfram Research, Inc.) to create the equations of motion for the three-mass tethered system is given in Appendix A.

The orbital period τ is calculated as

$$\tau = \frac{2\pi h^3}{\mu_e^2 (1 - \epsilon^2)^{\frac{3}{2}}} \tag{11}$$

where h is the angular momentum of the system and ϵ is the eccentricity of the orbit.

Nonlinear Control of Librational Motion

Delayed Feedback Control

Chaotic motion is characterized by bounded variation, sensitive dependence on initial conditions, and indivisibility such as transition on the phase plane. If a system is chaotic, it is generally possible for the trajectory of that system to fall into any number of bounded regions. Ott et al.[1] have shown that the chaotic system can be stabilized to a periodic solution with a period close to one of the bounded regions. Their method is called the OGY method. The delayed feedback control proposed by Pyragas[2] is used to calculate the control input using both the current output and the output delayed by one period as

$$u = K[\, y(\tau - t) - y(t)] \tag{12}$$

Figure 2 shows a block diagram of this method. This method can be interpreted as an extension of the OGY method to feedback control in continuous systems and has been studied to stabilize the librational motion of a tethered subsatellite system to a periodic solution with the same period as that of the orbit.[8,12] Very small external forces can have a large effect on the system dynamics because chaotic motion is very sensitive to initial conditions. In other words, the magnitude of the control input for delayed feedback control becomes small when the chaotic librational motion of the system is successfully stabilized to a periodic solution. This is an advantage of the delayed feedback control when applied to control chaotic motion. Another advantage of this method is that the method does not require preliminary calculation, other than the period, of the desired trajectory. Thus, this method is robust with respect to parameter variations.

Decoupling Control Method

A nonlinear differential equation in the affine form with respect to the control input is given by

$$\dot{\boldsymbol{x}} = f(\boldsymbol{x}) + \sum_{i=1}^{s} g_i(\boldsymbol{x}) u_i \qquad x \in R^n \tag{13}$$

$$\boldsymbol{y} = h(\boldsymbol{x}) \qquad \boldsymbol{y} \in R^p \tag{14}$$

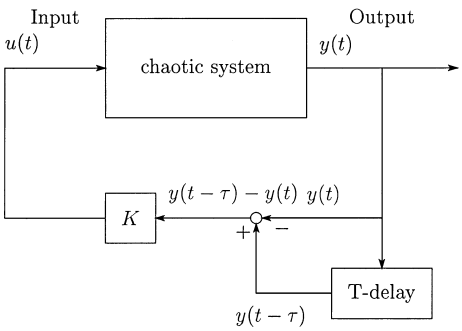

Fig. 2 Delayed feedback control method.

where $\boldsymbol{x}$, $\boldsymbol{y}$, and u are the state vector, output vector, and control input, respectively. We consider the problem of finding the nonlinear control input by which each output can be controlled independently. This problem is called the Morgan problem, in which the dimension of the output p is equal to that of the control input s. The transformation to obtain such a nonlinear control input is referred to as the decoupling method. We apply this method in order to control the tether angles θ_1 and θ_2 independently. The nonlinear control input to decouple the system is given by

$$\boldsymbol{u} = B^{-1}(\boldsymbol{x})[-a(\boldsymbol{x}) + \boldsymbol{v}] \tag{15}$$

$$a(\boldsymbol{x}) = \begin{bmatrix} L_f^{r_1} h_1(\boldsymbol{x}) \\ \cdots \\ L_f^{r_s} h_s(\boldsymbol{x}) \end{bmatrix} \tag{16}$$

$$B(\boldsymbol{x}) = \begin{bmatrix} L_{g_1} L_f^{r_1 - 1} h_1(\boldsymbol{x}) & \cdots & L_{g_s} L_f^{r_1 - 1} h_1(\boldsymbol{x}) \\ & \vdots & \\ L_{g_1} L_f^{r_s - 1} h_s(\boldsymbol{x}) & \cdots & L_{g_s} L_f^{r_s - 1} h_s(\boldsymbol{x}) \end{bmatrix} \tag{17}$$

where $\boldsymbol{v}$ is the fictitious control input and $L_f h(\boldsymbol{x})$ is the Lie derivative of $h(\boldsymbol{x})$ along f defined as

$$L_f h(\boldsymbol{x}) = \frac{\partial h}{\partial x} f(\boldsymbol{x}) \tag{18}$$

If $h(\boldsymbol{x})$ is differentiated $(i + 1)$ times along f, the notation $L_f^{i+1} h(\boldsymbol{x})$ is used as follows:

$$L_f^{i+1} h(x) = L_f L_f^i h(\boldsymbol{x}) \tag{19}$$

with $L_f^0 h(x) = h(\boldsymbol{x})$.

As the result of this control input, the system is decoupled as

$$\frac{\mathrm{d}^{r_k}}{\mathrm{d}t^{r_k}} y_k = v_k, \qquad k = 1, \ldots, s \tag{20}$$

where r_k is the relative degree to the output y_k and satisfies the condition

$$L_{g_j} L_f^{i-1} h_k(\boldsymbol{x}) \begin{cases} = 0 & (i < r_k, \quad \forall\, j = 1, \ldots, s) \\ \neq 0 & (i = r_k, \quad \exists\, j = 1, \ldots, s) \end{cases} \tag{21}$$

We show in Appendix B an implementation by Mathematica code to obtain the relative degree to the output and the nonlinear control input.

Let us apply the decoupling method to the tethered system shown in Fig. 1. The state vector of the system and the control inputs are, respectively, described as

$$[x_1, x_2, x_3, x_4, x_5, x_6, x_7, x_8]^T = [R_c, \eta, \theta_1, \theta_2, \dot{R}_c, \dot{\eta}, \dot{\theta}_1, \dot{\theta}_2]^T \tag{22}$$

$$[u_1,\ u_2]^T = [F_1,\ F_2]^T \tag{23}$$

The equation of motion is given in the form of Eq. (13), and the angles of the tethers are chosen as the outputs:

$$\begin{bmatrix} y_1 \\ y_2 \end{bmatrix} = \begin{bmatrix} h_1(t) \\ h_2(t) \end{bmatrix} = \begin{bmatrix} \theta_1(t) \\ \theta_2(t) \end{bmatrix} \tag{24}$$

The relative degrees of the system with respect to the outputs $h_1(t)$ and $h_2(t)$ and r_1 and r_2 are obtained as $r_1 = 2$ and $r_2 = 2$. Thus, we have the regular matrix

$$B(\boldsymbol{x}) = \begin{bmatrix} L_{g_1} L_f h_1(x) & L_{g_2} L_f h_1(x) \\ L_{g_1} L_f h_2(x) & L_{g_2} L_f h_2(x) \end{bmatrix} = \begin{bmatrix} B_{11} & B_{12} \\ B_{21} & B_{22} \end{bmatrix} \tag{25}$$

where

$$B_{11} = \frac{\cos x_3}{(m_0+m_1+m_2)x_1} - \frac{m_0+m_1+m_2\cos^2 x_4}{\left[m_0m_2\sin^2 x_4 + m_1(m_0+m_1+m_2)\right]l_1} \tag{26}$$

$$B_{12} = \frac{\cos(x_3+x_4)}{(m_0+m_1+m_2)x_1} \tag{27}$$

$$B_{21} = \frac{(m_0+m_1+m_2)l_1\cos x_4 + (m_0+m_1+m_2\cos^2 x_4)l_2}{\left[m_0m_2\sin^2 x_4 + m_1(m_0+m_1+m_2)\right]l_1l_2} \tag{28}$$

$$B_{22} = -\frac{1}{m_2l_2} \tag{29}$$

Employing the feedback control

$$[u_1 \quad u_2]^T = B^{-1}(\boldsymbol{x})[-a(\boldsymbol{x}) + \boldsymbol{v}]$$

$$= \begin{bmatrix} L_{g_1}L_f h_1(x) & L_{g_2}L_f h_1(x) \\ L_{g_1}L_f h_2(x) & L_{g_2}L_f h_2(x) \end{bmatrix}^{-1} \left(-\begin{bmatrix} L_f^2 h_1(x) \\ L_f^2 h_2(x) \end{bmatrix} + \begin{bmatrix} v_1 \\ v_2 \end{bmatrix} \right) \tag{30}$$

yields the decoupled system

$$\begin{bmatrix} \ddot{h}_1 \\ \ddot{h}_2 \end{bmatrix} = \begin{bmatrix} \ddot{\theta}_1 \\ \ddot{\theta}_2 \end{bmatrix} = \begin{bmatrix} v_1 \\ v_2 \end{bmatrix} \tag{31}$$

The angles of the tethers θ_1 and θ_2 can be independently controlled by the fictitious control inputs v_1 and v_2.

Model-Following, Decoupling-Control Method

The model-following control method is initially used to specify the reference model that behaves desirably, and later to control the response of a plant to converge asymptotically to that of the reference model by providing feedback control inputs based on the difference between responses. The model-following control law for the tethered satellite system in Fig. 1 will now be derived by combining the decoupling control method.[3]

Consider the plant model and the reference model described in the form of the affine differential equation:

$$\dot{\boldsymbol{x}}_P = f_P(\boldsymbol{x}_P) + g_P(\boldsymbol{x}_P)u_P \qquad \boldsymbol{x}_P \in R^{n_P}, \quad u_P \in R^r \tag{32}$$

$$\boldsymbol{y}_P = h_P(\boldsymbol{x}_P) \qquad y_P \in R^s \tag{33}$$

$$\dot{\boldsymbol{x}}_M = f_M(\boldsymbol{x}_M) + g_M(\boldsymbol{x}_M)u_M \qquad \boldsymbol{x}_M \in R^{n_M}, \quad u_M \in R^r \tag{34}$$

$$y_M = h_M(\boldsymbol{x}_M) \qquad y_M \in R^s \tag{35}$$

Note that $f_{Pi}(x_P)$, $g_{Pji}(x_P)$, $h_{Pk}(x_P)$ $(i=1,\ldots,n_P,\ j=1,\ldots,r,\ k=1,\ \ldots,s)$, $f_{Mi}(\boldsymbol{x}_M)$, $g_{Mji}(\boldsymbol{x}_M)$, and $h_{Mk}(\boldsymbol{x}_M)$ $(i=1,\ldots,n_M,\ j=1,\ldots,r, k=1,\ldots,s)$ are C^∞ functions, and $s \le r$.

The extended system combining the plant model and the reference model can be represented as

$$\dot{\boldsymbol{x}} = f(\boldsymbol{x}) + g(\boldsymbol{x})u \tag{36}$$

where $\boldsymbol{x} = [\boldsymbol{x}_P^T, \boldsymbol{x}_M^T]^T$, $\boldsymbol{u} = [\boldsymbol{u}_P^T, \boldsymbol{u}_M^T]^T$, $f(\boldsymbol{x}) = [f_P(\boldsymbol{x}_P)^T,\ f_M(\boldsymbol{x}_M)^T]^T$, and

$$g(\boldsymbol{x}) = [g_1(\boldsymbol{x}), g_2(\boldsymbol{x})] = \begin{bmatrix} g_P(\boldsymbol{x}_P) & 0 \\ 0 & g_M(\boldsymbol{x}_M) \end{bmatrix}$$

The difference between the output of the reference model and that of the plant

$$h(\boldsymbol{x}) = e = h_M(\boldsymbol{x}_M) - h_P(\boldsymbol{x}_P) \tag{37}$$

is treated as the output of the preceding extended system.

Let us consider the case in which the plant is controlled by

$$\boldsymbol{u}_P = \alpha(\boldsymbol{x}) + \beta(\boldsymbol{x})\boldsymbol{u}_M \tag{38}$$

and the reference model is controlled by the arbitrary control input u_M. In this case, if the error e asymptotically converges to zero as time increases the plant can be regarded as following the reference model.

We refer to the relative degrees of $h_{Pi}(\boldsymbol{x}_P)$ and $h_{Mi}(\boldsymbol{x}_M)$ $(i=1,\ldots,s)$ as p_i and π_i, respectively, and consider the following matrices:

$$Q_P(\boldsymbol{x}_P) = \begin{bmatrix} L_{g_P}L_{f_P}^{p_1-1}h_{P1} \\ \vdots \\ L_{g_P}L_{f_P}^{p_s-1}h_{Ps} \end{bmatrix}$$

$$= \begin{bmatrix} L_{g_{P1}}L_{f_P}^{p_1-1}h_{P1} & \cdots & L_{g_{Pr}}L_{f_P}^{p_1-1}h_{P1} \\ \vdots & \ddots & \vdots \\ L_{g_{P1}}L_{f_P}^{p_s-1}h_{Ps} & \cdots & L_{g_{Pr}}L_{f_P}^{p_s-1}h_{Ps} \end{bmatrix} \tag{39}$$

$$Q_M(\boldsymbol{x}_M) = \begin{bmatrix} L_{g_M}L_{f_M}^{p_1-1}h_{M1} \\ \vdots \\ L_{g_M}L_{f_M}^{p_s-1}h_{Ms} \end{bmatrix}$$

$$= \begin{bmatrix} L_{g_{M1}}L_{f_M}^{p_1-1}h_{M1} & \cdots & L_{g_{Mr}}L_{f_M}^{p_1-1}h_{M1} \\ \vdots & \ddots & \vdots \\ L_{g_{M1}}L_{f_M}^{p_s-1}h_{Ms} & \cdots & L_{g_{Mr}}L_{f_M}^{p_s-1}h_{Ms} \end{bmatrix} \tag{40}$$

When the rank of the matrix $Q_P(\boldsymbol{x}_P)$ is full, the necessary and sufficient condition for the existence of the control law, Eq. (38), is as follows:

$$p_k \le \pi_k \qquad k = 1,\ldots,s \tag{41}$$

To obtain the control law [Eq. (38)] by which the response of the plant is controlled to asymptotically converge to that of the reference model, we need to find the functions $\alpha(x)$ and $\beta(x)$ that satisfy

$$Q_P(\boldsymbol{x}_P)\alpha(\boldsymbol{x}) = \begin{bmatrix} L_{f_M}^{p_1}h_{M1} \\ \vdots \\ L_{f_M}^{p_s}h_{Ms} \end{bmatrix} - \begin{bmatrix} L_{f_P}^{p_1}h_{P1} \\ \vdots \\ L_{f_P}^{p_s}h_{Ps} \end{bmatrix} + \boldsymbol{z} \tag{42}$$

$$Q_P(\boldsymbol{x}_P)\beta(\boldsymbol{x}) = Q_M(\boldsymbol{x}_M) \tag{43}$$

where $\boldsymbol{z}$ is a vector with s dimension, and each element of which z_k is a function of

$$e_j^{(i)} = L_{f_M}^i h_{Mj} - L_{f_P}^i h_{Pj} \qquad i = 0,\ldots,p_j-1, \quad j = 1,\ldots,s \tag{44}$$

In this case the following relationship is satisfied:

$$e_k^{(p_k)} = L_{f_M}^{p_k}h_{Mk} + L_{G_M}L_{f_M}^{p_k-1}h_{Mk}u_M - L_{f_P}^{p_k}h_{Pk}$$

$$- L_{G_P}L_{f_P}^{p_k-1}h_{Pk}[\alpha(\boldsymbol{x}) + \beta(\boldsymbol{x})u_M] = -z_k \tag{45}$$

If we choose the vector

$$\hat{e} = \left[e_1,\ldots,e_1^{(p_1-1)}, e_2,\ldots,e_2^{(p_2-1)},\ldots,e_m,\ldots,e_m^{(p_s-1)}\right]^T \tag{46}$$

and define z_k using $\hat{e}$ and a constant vector f_k as

$$z_k = f_k^T\hat{e} \tag{47}$$

the poles of the output of the extended system can be set arbitrarily.

Let us apply the preceding formulation to the three-mass tethered satellite system (Fig. 1) in an elliptic orbit. The tethered satellite system in an elliptic orbit is considered to be controlled as the plant model.

Although the tethered satellite system in an elliptic orbit can be used as the reference model when the motion of the system has been changed to an adequate degree to periodic motion by the control, in order to simplify the problem the formulation is shown only for the case in which the reference model is represented by the motion of the tethered satellite system in a circular orbit. The formulation for the case in which the reference motion is represented as the motion in an elliptic orbit is not shown in this section because this motion is basically identical to the motion already explained. The results of numerical simulations for both cases will be presented in the following section.

The state vector and control inputs and outputs of the plant model [Eq. (32)] are given by

$$\boldsymbol{x}_P = \left[x_{P1}, \ldots, x_{P8}\right]^T = [R_c, \eta, \theta_1, \theta_2, \dot{R}_c, \dot{\eta}, \dot{\theta}_1, \dot{\theta}_2]^T \in \boldsymbol{R}^8 \quad (48)$$

$$\boldsymbol{u}_P = \left[u_{P1}, u_{P2}\right]^T = [F_1, F_2]^T \in \boldsymbol{R}^2 \quad (49)$$

$$\boldsymbol{y}_P = \left[y_{P1}, y_{P2}\right]^T = [\theta_1, \theta_2]^T = \left[x_{P1}, x_{P2}\right]^T \in \boldsymbol{R}^2 \quad (50)$$

Similarly, the state vector and control inputs and outputs of the reference model that is the tethered satellite system in a circular orbit are given by

$$\boldsymbol{x}_M = \left[x_{M1}, \ldots, x_{M4}\right]^T = [\theta_1, \theta_2, \dot{\theta}_1, \dot{\theta}_2]^T \in \boldsymbol{R}^4 \quad (51)$$

$$\boldsymbol{u}_M = \left[u_{M1}, u_{M2}\right]^T = [F_1, F_2]^T \in \boldsymbol{R}^2 \quad (52)$$

$$\boldsymbol{y}_M = \left[y_{M1}, y_{M2}\right]^T = [\theta_1, \theta_2]^T = \left[x_{M1}, x_{M2}\right]^T \in \boldsymbol{R}^2 \quad (53)$$

In this case the relative degrees of the plant model and the reference model are obtained as $p_1 = p_2 = 2$ and $\pi_1 = \pi_2 = 2$, respectively. This means that the necessary and sufficient condition for the existence of the control law, Eq. (41), is satisfied. The matrices $Q_P(\boldsymbol{x}_P)$ and $Q_M(\boldsymbol{x}_M)$ for the preceding models are obtained, respectively, as follows:

$$Q_P(\boldsymbol{x}_P) = \begin{bmatrix} L_{g_{P1}} L^1_{f_P} h_{P1} & L_{g_{P2}} L^1_{f_P} h_{P1} \\ L_{g_{P1}} L^1_{f_P} h_{P2} & L_{g_{P2}} L^1_{f_P} h_{P2} \end{bmatrix} = \begin{bmatrix} Q_{P11} & Q_{P12} \\ Q_{P21} & Q_{P22} \end{bmatrix} \quad (54)$$

where

$$Q_{P11} = \frac{\cos x_{P3}}{(m_0 + m_1 + m_2) x_{P1}} - \frac{m_0 + m_1 + m_2 \cos^2 x_{P4}}{\left[m_0 m_2 \sin^2 x_{P4} + m_1 (m_0 + m_1 + m_2)\right] l_1} \quad (55)$$

$$Q_{P12} = \frac{\cos\left(x_{P3} + x_{P4}\right)}{(m_0 + m_1 + m_2) x_{P1}} \quad (56)$$

$$Q_{P21} = \frac{(m_0 + m_1 + m_2) l_1 \cos x_{P4} + \left(m_0 + m_1 + m_2 \cos^2 x_{P4}\right) l_2}{\left[m_0 m_2 \sin^2 x_{P4} + m_1 (m_0 + m_1 + m_2)\right] l_1 l_2} \quad (57)$$

$$Q_{P22} = -\frac{1}{m_2 l_2} \quad (58)$$

$$Q_M(x_M) = \begin{bmatrix} L_{g_{M1}} L^1_{f_M} h_{M1} & L_{g_{M2}} L^1_{f_M} h_{M1} \\ L_{g_{M1}} L^1_{f_M} h_{M2} & L_{g_{M2}} L^1_{f_M} h_{M2} \end{bmatrix} = \begin{bmatrix} Q_{M11} & Q_{M12} \\ Q_{M21} & Q_{M22} \end{bmatrix} \quad (59)$$

where

$$Q_{M11} = -\frac{\left(m_0 + m_1 + m_2 \cos^2 x_{M2}\right) R_c^3}{\mu_e \left[m_0 m_2 \sin^2 x_{M2} + m_1 (m_0 + m_1 + m_2)\right] l_1} \quad (60)$$

$$Q_{M12} = 0 \quad (61)$$

$$Q_{M21} = \frac{\left[(m_0 + m_1 + m_2) l_1 \cos x_{M2} + \left(m_0 + m_1 + m_2 \cos^2 x_{M2}\right) l_2\right] R_c^3}{\mu_e \left[m_0 m_2 \sin^2 x_{M2} + m_1 (m_0 + m_1 + m_2)\right] l_1 l_2} \quad (62)$$

$$Q_{M22} = -\frac{R_c^3}{\mu_e m_2 l_2} \quad (63)$$

The matrices $Q_P(\boldsymbol{x}_P)$ and $Q_M(\boldsymbol{x}_M)$ are full rank matrices. Therefore, the nonlinear control law, Eq. (38), can be obtained by substituting the preceding equations into Eqs. (42) and (43) and solving these equations with respect to the functions $\alpha(\boldsymbol{x})$ and $\beta(\boldsymbol{x})$. The resulting functions $\alpha(\boldsymbol{x})$ and $\beta(\boldsymbol{x})$ are

$$\alpha(\boldsymbol{x}) = Q_P(\boldsymbol{x}_P)^{-1} \left[\begin{bmatrix} L^{p_1}_{f_M} h_{M1} \\ \vdots \\ L^{p_s}_{f_M} h_{Ms} \end{bmatrix} - \begin{bmatrix} L^{p_1}_{f_P} h_{P1} \\ \vdots \\ L^{p_s}_{f_P} h_{Ps} \end{bmatrix} + z \right] \quad (64)$$

$$\beta(\boldsymbol{x}) = Q_P(\boldsymbol{x}_P)^{-1} Q_M(\boldsymbol{x}_M) \quad (65)$$

Because the relative degrees p_1, p_2, π_1, and π_2 are equal to 2, as mentioned before, the following PD feedback control can be employed.

$$z_1 = K_{P1} e_1 + K_{D1} \dot{e}_1 \quad (66)$$

$$z_2 = K_{P2} e_2 + K_{D2} \dot{e}_2 \quad (67)$$

As the result of the preceding feedback control, we have

$$\ddot{e}_1 = -z_1 = -K_{P1} e_1 - K_{D1} \dot{e}_1 \quad (68)$$

$$\ddot{e}_2 = -z_2 = -K_{P2} e_2 - K_{D2} \dot{e}_2 \quad (69)$$

where K_{P1}, K_{D1}, K_{P2}, and K_{D2} are constant control gains. As mentioned earlier, the poles of the decoupled system can be chosen arbitrarily by setting the preceding control gains.

Numerical Simulations

In the present study we assume the masses of the mother satellite and each subsatellite to be 50,000 and 500 kg, respectively, and assume the length of each tether to be 50 km.

We conduct three types of simulations in order to demonstrate the validity of each control method described in the preceding section. Although the orbital period is influenced by the gravity-gradient force and the thruster jets for controlling libration of the system, for the sake of simplicity the orbital period obtained by substituting the initial state into Eq. (11) is used to generate the delayed output signal.

Lyapunov Exponent

The tethered subsatellite oscillates in opposition to the mother satellite as a random pendulum caused by the gravity-gradient force if the eccentricity of the system is less than approximately 0.3. This motion is called librational motion and becomes chaotic as the eccentricity of the system becomes large and easily undergoes transition to circular motion if the eccentricity of the system is greater than approximately 0.3. The significance of this value of the eccentricity is explained in this subsection using Lyapunov exponents.[14] Values of the eccentricity for numerical simulations in later subsections are chosen to be less than 0.3 so that the three-mass tethered

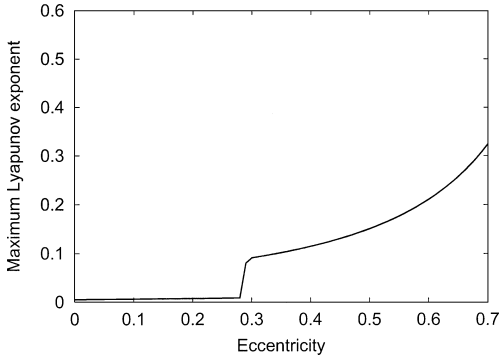

Fig. 3 Maximum Lyapunov exponent with respect to eccentricity.

satellite system does not easily undergo transition to circular motion but behaves with chaotic, librational motion. This is necessary because the librational motion is more suitable for conducting scientific missions than the circular motion.

The Lyapunov exponent is the averaged rate of divergence (or convergence) of two neighboring trajectories for chaotic systems. The Lyapunov exponent has a whole spectrum in accordance with the degree of freedom of the system. To explain the spectrum related to the Lyapunov exponent, let us consider a small ball with radius dr, which includes the initial condition. This small ball is deformed into an ellipsoid over time. The ith Lyapunov exponent is defined as

$$\lambda_i = \lim_{t\to\infty} \frac{1}{t} \ell_n \left(\frac{dw_i}{dr} \right) \tag{70}$$

where dw_i is the ith radius of the ellipsoid along its ith principal axis. We used the number of orbits as the denominator to calculate the Lyapunov exponent instead of the real time in the present study. The largest exponent is most commonly referred to as the Lyapunov exponent. A positive Lyapunov exponent indicates that the predictability of the future status of the system quickly vanishes with time. If the Lyapunov exponent undergoes a sudden or dramatic increase, the system trajectory moves into a new chaotic realm, in which the trajectory is more sensitive to the initial conditions.

Figure 3 shows the Lyapunov exponent with respect to the eccentricity of the tethered satellite system treated in the present study. The Lyapunov exponent is a stable, small positive value when the eccentricity is small. Even if the eccentricity is zero, the Lyapunov exponent of the tethered satellite system treated in the present paper is not zero. This is because the three-mass tethered satellite system has two degrees of freedom as tether angles and, as a result, is a nonlinear chaotic system. The exponent dramatically increases at an eccentricity of approximately 0.3. This change in the Lyapunov exponent indicates that the tethered subsatellite system of the present study behaves more chaotically and exhibits circular motion when the eccentricity is greater than approximately 0.3. This value of the eccentricity depends slightly on the ratio of the mass of the subsatellite to that of the mother satellite.

Results of the Delayed Feedback Control

The initial states of the system are given as follows: $R_c = 6600$ km, $\eta = 0$, $\theta_1 = \pi$ rad, $\theta_2 = 0.2$ rad, $\dot{R}_c = 0$ km/s, $\dot{\eta} = 1.28994 \times 10^{-3}$ rad/s, and $\dot{\theta}_1 = \dot{\theta}_2 = 0$ rad/s. The orbital period based on the initial states τ is determined, based on Eq. (11), to be 7457s, and the eccentricity of the mass center of the system is found to be 0.2. In the present simulation $\dot{\theta}_1$ is measured as the output of the system and only thruster 1 is employed to control θ_1 so that the oscillation period of θ_1 becomes the same as the orbital period based on the initial states (7457 s). The magnitude of thrust from thruster 1 is calculated by Eq. (12), where the control gain for the delayed feedback control K is set as $-4.0 \times 10^4 \pi/\tau$ N · s/rad.

The time responses of tether angles θ_1 and θ_2 are shown in Figs. 4 and 5. These figures show that tether angles oscillate randomly at first, but become periodic after a sufficiently long time as a result

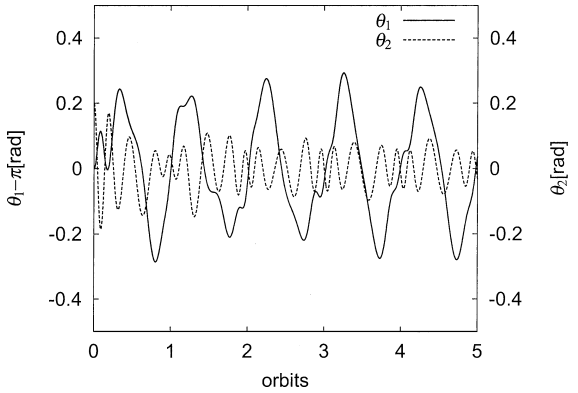

Fig. 4 Time response of the tether angles controlled by delayed feedback control.

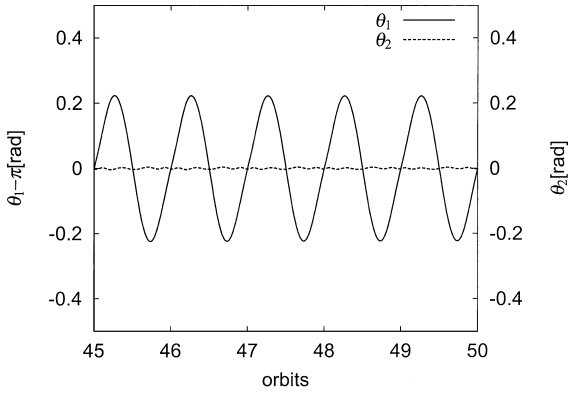

Fig. 5 Time response of the tether angles after adequately stabilized by delayed feedback control.

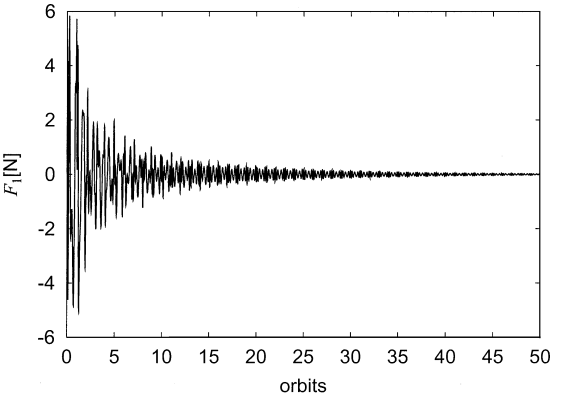

Fig. 6 Time response of thruster 1.

of the action of the delayed feedback control. This result shows that the delayed feedback control can eliminate chaotic motion but not librational motion. Therefore, if the elimination of librational motion is required the combination of the delayed feedback control with some sort of control scheme will be necessary.

The time response of thruster 1 is shown in Fig. 6, which shows that the magnitude of the control input is small after the state is adequately stabilized to a periodic solution. However a long time (about 50 orbits) is required before reaching a periodic motion.

Results of the Decoupling-Control Method

The equilibrium point for the system in a circular orbit, $(\theta_1, \theta_2) = (\pi, 0)$, is selected as the reference angles. The initial states of the system are chosen as the preceding simulation, that is, $R_c(0) = 6600$ km, $\eta(0) = 0$, $\theta_1(0) = \pi$ rad, $\theta_2(0) = 0.2$ rad, $\dot{R}_c(0) = 0$ km/s, $\dot{\eta}(0) = 1.28994 \times 10^{-3}$ rad/s, and $\dot{\theta}_1(0) = \dot{\theta}_2(0) = 0$ rad/s.

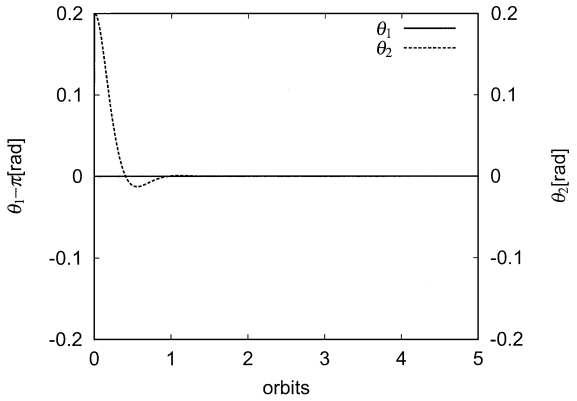

Fig. 7 Time responses of the tether angles for the decoupling control method.

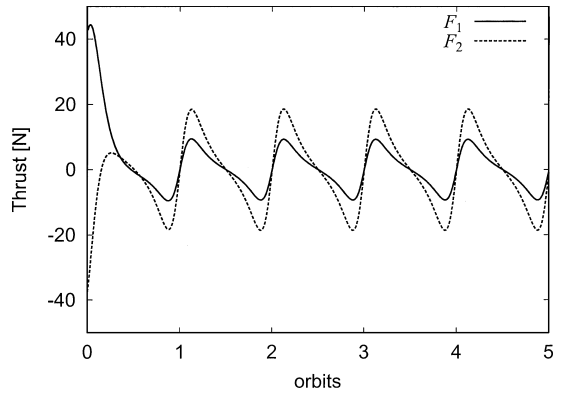

Fig. 8 Time responses of the thrusts for the decoupling control method.

The orbital period of the system τ is the same as that of the preceding simulation (7451 s). To achieve the reference angles, the following PD-type feedback control is chosen for generating the fictitious control inputs in Eq. (31), v_1 and v_2:

$$v_1 = -K_{P1}(\theta_1 - \pi) - K_{D1}\dot{\theta}_1, \qquad v_2 = -K_{P2}\theta_2 - K_{D2}\dot{\theta}_2$$

The control gains are set as $K_{P1} = K_{P2} = -0.01/\tau \text{ s}^{-2}$, $K_{D1} = -1/\tau \text{ s}^{-1}$, and $K_{D2} = -13.0/\tau \text{ s}^{-1}$ in the present simulation. The time responses of the tether angles are shown in Fig. 7, which shows that the tether angle θ_2 is successfully controlled by the decoupling method without any changes in the tether angle θ_1. The time responses of the thrusters are shown in Fig. 8. The magnitude of the thruster becomes small after the tether angles converge to the reference angles, but does not become zero because the reference angles are the equilibrium angles for the system in a circular orbit and the plant model is controlled in an elliptic orbit.

Results of the Model-Following, Decoupling-Control Method

Case 1: Reference Model in a Circular Orbit

The tethered satellite system in a circular orbit with the radius 8250 km is treated as the reference model. The orbital period of this reference model is 7457 s. The plant model is assumed to be the tethered satellite system in an elliptic orbit with eccentricity $\epsilon = 0.2$ and radius of perigee = 6600 km. The orbital period of this plant at the initial time is the same as that of the reference model (7457 s). The control gains are set as $K_{P1} = K_{P2} = 2.0 \times 10^{-4}\pi/\tau \text{ s}^{-2}$ and $K_{D1} = K_{D2} = 0.8\pi/\tau \text{ s}^{-1}$. The reference system is given by $\theta_1(0) = (\pi + 0.01)$ rad, $\theta_2(0) = 0$ rad, and $\dot{\theta}_1(0) = \dot{\theta}_2(0) = 0$ rad/s at the initial time, and no control is used to actuate the reference system, that is, $\boldsymbol{u}_M = 0$. The initial tether angles of the reference model are small deviations from the equilibrium angles because the three-mass tethered satellite system is basically chaotic, even if the system is in a circular orbit. Thus, the system without control does not oscillate periodically unless small tether angles are given to the system at the initial time. The plant is given the radius $R_c = 6600$ km, $\eta = 0$ rad; the tether angles $\theta_1(0) = \pi$ rad, $\theta_2(0) = 0.2$ rad; and tether angular velocities $\dot{\theta}_1(0) = 0$ rad/s, $\dot{\theta}_2(0) = 0$ rad/s at the initial time.

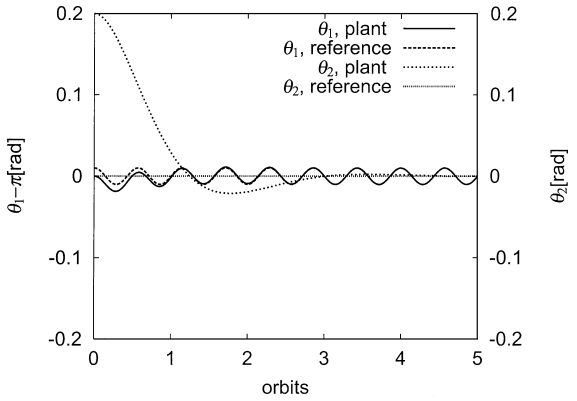

Fig. 9 Time responses of the tether angles for the model-following, decoupling-control method for the reference model in circular orbit.

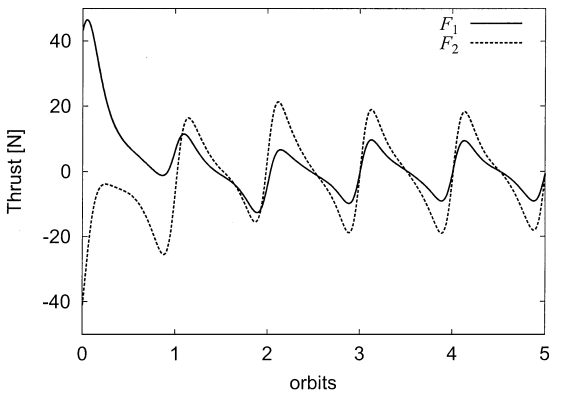

Fig. 10 Time responses of the thrusts for the model-following, decoupling-control method for the reference model in circular orbit.

The oscillations of the tether angles of the reference model are almost sinusoidal waves, as shown in Fig. 9. The period of oscillation of the reference model is $\tau/\sqrt{3}$, that is, 4305 s. The time response of the plant controlled to follow the motion of the reference model and that of the reference model are shown in Fig. 9. This figure shows that the response of the plant model successfully follows that of the reference model and that the errors converge to zero within about four orbital periods. The time responses of the control inputs are shown in Fig. 10. The magnitudes of the thrusters do not become zero, and continuous large forces are required, even after the errors become zero because the orbit of the plant model, which is elliptic, is different from that of the reference model, which is circular. Therefore, the reference model in a circular orbit cannot be employed as the reference to follow even if the orbital period is the same as that of the tethered satellite system in an elliptic orbit.

Case 2: Reference Model in an Elliptic Orbit

When the delayed feedback is employed to control the tether angles, a rather lengthy time is required before the state takes on stabilized period motion. Similarly, when the periodic motion of the system in a circular orbit is employed as the reference motion for the system in an elliptic orbit a sufficiently long time is still needed until the motion of the plant model converges to the periodic solution. To improve this situation, let us replace the reference model with another model in the same elliptic orbit as the plant system, which is adequately stabilized by the delayed feedback control before being followed by the plant model, and let us consider that the plant model is controlled to follow this new reference model. The required time for convergence of the plant motion to the reference motion is expected to be reduced, and the periodic motion is expected to be achievable by small control inputs. This is because the reference

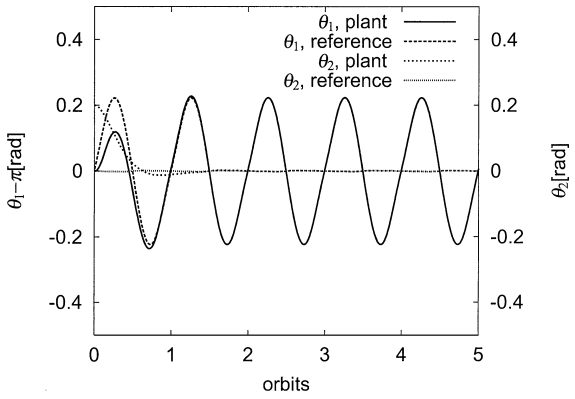

Fig. 11 Time responses of the tether angles for the model-following, decoupling-control method for the reference model in elliptic orbit.

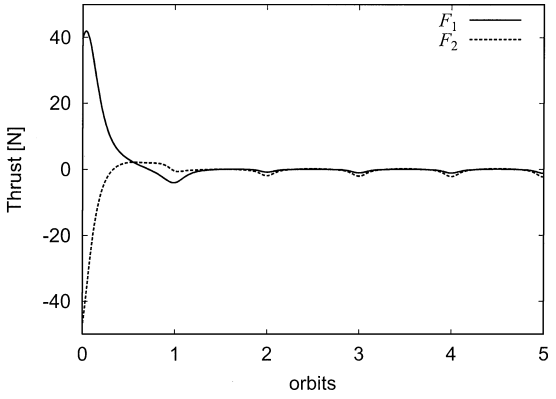

Fig. 12 Time responses of the thrusts for the model-following, decoupling-control method for the reference model in elliptic orbit.

model and plant model are now in the same elliptical orbit, with the same chaotic behavior. That is, once the librational motion of the plant model exactly match the reference model, they could remain virtually identical with almost no control effort because their chaotic nature is small for the case of eccentricity $= 0.2$, as shown in Fig. 3, and the periodic motion of the reference model is evidently maintained by the delayed feedback control of small control inputs, as shown in Fig. 6. Thus, the control must exert large forces for only a short time required to align plant librational motion with reference librational motion. The initial conditions for the plant model and control gains are set to the same values as in the preceding case.

The time responses of the tether angles and thrusters are shown in Figs. 11 and 12, respectively. The tether angles are controlled to follow the reference trajectory within about two orbital periods. This time is much shorter than that for the previous case, that is, four orbital periods. The thrusters are almost always zero after errors between response of the plant model and the reference model converge to zero, with the thrusters being only lightly operated when the plant system returns to the perigee. The time response of the thrusters resembles that of the control scheme proposed by Takeichi et al.,[12] which applies an impulsive force to the subsatellite of a dumbbell tethered satellite system in order to achieve the periodic oscillation of the system.

These results demonstrate that even though the tethered satellite system might have been launched into an elliptic orbit, if the eccentricity of the orbit is small, the tethered satellite system can be employed for low atmospheric Earth observation every orbital period.

Conclusions

A method to control libration of a tethered subsatellite system for an elliptical orbit has been proposed. The tethered subsatellite is modeled as a system consisting of a mother satellite and two subsatellites with thrusters, connected by massless and nonflexibe tethers, and only in-plane motion is studied. The delayed feedback control method using the thruster on the middle subsatellite can stabilize the chaotic, librational motion of the system to a periodic motion. The magnitude of the control input to maintain the stability of the system is small, whereas the time required in order to reach the periodic state is large. The decoupling method based on differential geometric control theory is studied to control the tether angles independently. If this motion is realized for the three-mass tethered satellite system, some scientific missions will be achieved such as the observation of meteors and aurora from more than two directions simultaneously, and the applications of the tethered system will be extended more. The model-following, decoupling-control method is applied such that either the librational motion of the tethered satellite in an elliptic orbit can track the periodic motion of the reference system in a circular orbit or it can track the reference system in an elliptic orbit that is adequately controlled by the delayed feedback control. The numerical simulations show that the reference system in a circular orbit cannot be employed as the reference model to follow even if the orbital period of the reference system is the same as that of the plant system in an elliptic orbit because continuous large control forces are required to track a periodic motion of the reference system in a circular orbit. The numerical simulations also illustrate that the proposed control method combining three control techniques has good performance such as a short settling time for convergence of the plant motion to the reference periodic motion and small control forces for maintaining the periodic motion of the plant system, for the case where the reference system and the plant system are in the same elliptical orbit.

Appendix A: Mathematica Code I

Mathematica code for obtaining the equations of motion of the three-mass tethered satellite system appears below. This code was implemented by M. Iwasaki.

```
avec[1] = {1, 0, 0};
avec[2] = {0, 1, 0};
lvec[1] = l[1]*(Cos[theta[1][t]]*avec[1] + Sin[theta[1][t]]*avec[2]);
lvec[2] = l[2]*((Cos[theta[1][t] + theta[2][t]])*avec[1]
     + (Sin[theta[1][t] + theta[2][t]])*avec[2]);
Rcvec[t] = Rc[t]*avec[1];
Rvec[0][t] = Rcvec[t] - (m[1] + m[2])/(m[0] + m[1] + m[2])*lvec[1]
     - (m[2])/(m[0] + m[1] + m[2])*lvec[2];
Rvec[1][t] = Rvec[0][t] + lvec[1];
Rvec[2][t] = Rvec[1][t] + lvec[2];
Rvec[0]'[t] = D[Rvec[0][t], t] + Cross[{0, 0, eta'[t]}, Rvec[0][t]];
Rvec[1]'[t] = D[Rvec[1][t], t] + Cross[{0, 0, eta'[t]}, Rvec[1][t]];
```

```
Rvec[2]'[t] = D[Rvec[2][t], t] + Cross[{0, 0, eta'[t]}, Rvec[2][t]];
Rvec[0]''[t] = D[Rvec[0]'[t], t] + Cross[{0, 0, eta'[t]}, Rvec[0]'[t]];
Rvec[1]''[t] = D[Rvec[1]'[t], t] + Cross[{0, 0, eta'[t]}, Rvec[1]'[t]];
Rvec[2]''[t] = D[Rvec[2]'[t], t] + Cross[{0, 0, eta'[t]}, Rvec[2]'[t]];
(* partial velocity *)
pvvec[0][1] = Coefficient[Rvec[0]'[t], Rc'[t]];
pvvec[0][2] = Coefficient[Rvec[0]'[t], eta'[t]];
pvvec[0][3] = Coefficient[Rvec[0]'[t], theta[1]'[t]];
pvvec[0][4] = Coefficient[Rvec[0]'[t], theta[2]'[t]];
pvvec[1][1] = Coefficient[Rvec[1]'[t], Rc'[t]];
pvvec[1][2] = Coefficient[Rvec[1]'[t], eta'[t]];
pvvec[1][3] = Coefficient[Rvec[1]'[t], theta[1]'[t]];
pvvec[1][4] = Coefficient[Rvec[1]'[t], theta[2]'[t]];
pvvec[2][1] = Coefficient[Rvec[2]'[t], Rc'[t]];
pvvec[2][2] = Coefficient[Rvec[2]'[t], eta'[t]];
pvvec[2][3] = Coefficient[Rvec[2]'[t], theta[1]'[t]];
pvvec[2][4] = Coefficient[Rvec[2]'[t], theta[2]'[t]];
(* Kane's equation *)
eqnofm =
     {-m[0]*Rvec[0]''[t].pvvec[0][1]
     -m[1]*Rvec[1]''[t].pvvec[1][1]
     -m[2]*Rvec[2]''[t].pvvec[2][1]
     -(mu*m[0]*Rvec[0][t]/((Rvec[0][t].Rvec[0][t])^(3/2))).pvvec[0][1]
     -(mu*m[1]*Rvec[1][t]/((Rvec[1][t].Rvec[1][t])^(3/2))).pvvec[1][1]
     -(mu*m[2]*Rvec[2][t]/((Rvec[2][t].Rvec[2][t])^(3/2))).pvvec[2][1]
     +F[1]*(Cos[theta[1][t] + Pi/2]*avec[1]
       +Sin[theta[1][t] + Pi/2]*avec[2]).pvvec[1][1]
     +F[2]*(Cos[theta[1][t] + theta[2][t] + Pi/2]*avec[1]
        +Sin[theta[1][t] + theta[2][t] + Pi/2]*avec[2]).pvvec[2][1] == 0,
     -m[0]*Rvec[0]''[t].pvvec[0][2]
     -m[1]*Rvec[1]''[t].pvvec[1][2]
     -m[2]*Rvec[2]''[t].pvvec[2][2]
     -(mu*m[0]*Rvec[0][t]/((Rvec[0][t].Rvec[0][t])^(3/2))).pvvec[0][2]
     -(mu*m[1]*Rvec[1][t]/((Rvec[1][t].Rvec[1][t])^(3/2))).pvvec[1][2]
     -(mu*m[2]*Rvec[2][t]/((Rvec[2][t].Rvec[2][t])^(3/2))).ppvec[2][2]
     +F[1]*(Cos[theta[1][t] + Pi/2]*avec[1]
        +Sin[theta[1][t] + Pi/2]*avec[2]).pvvec[1][2]
     +F[2]*(Cos[theta[1][t] + theta[2][t] + Pi/2]*avec[1]
        + Sin[theta[1][t] + theta[2][t] + Pi/2]*avec[2]).pvvec[2][2] == 0,
     -m[0]*Rvec[0]''[t].pvvec[0][3]
     -m[1]*Rvec[1]''[t].pvvec[1][3]
     -m[2]*Rvec[2]''[t].pvvec[2][3]
     -(mu*m[0]*Rvec[0][t]/((Rvec[0][t].Rvec[0][t])^(3/2))).pvvec[0][3]
     -(mu*m[1]*Rvec[1][t]/((Rvec[1][t].Rvec[1][t])^(3/2))).ppvec[1][3]
     -(mu*m[2]*Rvec[2][t]/((Rvec[2][t].Rvec[2][t])^(3/2))).pvvec[2][3]
     +F[1]*(Cos[theta[1][t] + Pi/2]*avec[1]
        +Sin[theta[1][t] + Pi/2]*avec[2]).pvvec[1][3]
     +F[2]*(Cos[theta[1][t] + theta[2][t] + Pi/2]*avec[1]
        +Sin[theta[1][t] + theta[2][t] + Pi/2]*avec[2]).pvvec[2][3] == 0,
     -m[0]*Rvec[0]''[t].pvvec[0][4]
     -m[1]*Rvec[1]''[t].pvvec[1][4]
     -m[2]*Rvec[2]''[t].pvvec[2][4]
```

```
     -(mu*m[0]*Rvec[0][t]/((Rvec[0][t].Rvec[0][t])^(3/2))).pvvec[0][4]
     -(mu*m[1]*Rvec[1][t]/((Rvec[1][t].Rvec[1][t])^(3/2))).pvvec[1][4]
     +F[1]*(Cos[theta[1][t] + Pi/2]*avec[1]
        +Sin[theta[1][t] + Pi/2]*avec[2]).pvvec[1][4]
     -(mu*m[2]*Rvec[2][t]/((Rvec[2][t].Rvec[2][t])^(3/2))).pvvec[2][4]
     +F[2]*(Cos[theta[1][t] + theta[2][t] + Pi/2]*avec[1]
        +Sin[theta[1][t] + theta[2][t] + Pi/2]*avec[2]).pvvec[2][4] == 0};

sol = Solve[eqnofm, {Rc''[t], eta''[t], theta[1]''[t], theta[2]''[t]}];
(* Equations of motion, where x[i] is a state variable vector. *)
f0 = {x[5],
     x[6],
     x[7],
     x[8],
     (rc''[t] /. sol)[[1]] ,
     (eta''[t] /. sol)[[1]],
     (theta[1]''[t] /. sol)[[1]],
     (theta[2]''[t] /. sol)[[1]]};
(* the nonlinear differential equation in the affine form *)
f = Coefficient[Coefficient[f0, F[1], 0], F[1], 0];
g[1] = Coefficient[f0, F[1]];
g[2] = Coefficient[f0, F[2]];
```

Appendix B: Mathematica Code II

Mathematica code for obtaining the relative degree and nonliner control input for the decoupling control based on the differential control theory, where n, s, and p are the dimension of the state variable vector, the dimension of the control input, and the dimension of the output, respectively:

```
n = 8; p = 2;
output[1] = x[3];
output[2] = x[4];
(* Function lieD is the Lie derivative of scalar function phi
  with respect to vector field f. *)
lieD[f_, phi_] := Table[D[phi, x[i]], {i, 1, n}].f
(* lieDalongF function is defined by combining lieD
  with Mathematica function Nest. *)
lieDalongF[phi_] := lieD[f, phi];
(* The relative degree r[k] is calculated. *)
Do[r[k] =
  {i = 1;
    While[
      Apply[And,
      Table[(lieD[g[j], Nest[lieDalongF, output[k], i - 1]] == 0),
        {j,1, p}]],
    i++];
  i}[[1]], {k, 1, p}];

(* The control inputs for decoupling, u, are obtained
  for the case p = s. *)
beta = Table[lieD[g[j], Nest[lieDalongF, output[i], r[i] - 1]],
    {i, 1, p}, {j, 1, p}];
alpha = Table[Nest[lieDalongF, output[i], r[i]], {i, 1, p}];
u = -Inverse[beta].alpha + Inverse[beta].Table[v[i], {i, 1, p}];
```

References

[1]Ott, E., Grebogi, C., and Yorke, Y. A., "Controlling Chaos," *Physical Review Letters*, Vol. 64, No. 11, 1990, pp. 1196–1199.

[2]Pyragas, K., "Continuous Control of Chaos by Self-Controlling Feedback," *Physics Letters A*, Vol. 170, No. 6, 1992, pp. 421–428.

[3]Isidori, A., *Nonlinear Control Systems*, 3rd ed., Springer-Verlag, New York, 1995, Chap. 5.

[4]Schechter, H. B., "Dumbbell Librations in Elliptic Orbits," *AIAA Journal*, Vol. 2, No. 6, 1964, pp. 1000–1003.

[5]Karasopoulos, H. A., and Richardson, D. L., "Chaos in the Pitch Equation of Motion of the Gravity-Gradient Satellite," AIAA Paper 92-4369, 1992.

[6]Karasopoulos, H. A., and Richardson, D. L., "Numerical Investigation of Chaos in the Attitude Motion of a Gravity-Gradient Satellite," *Astrodynamics 1993*, Vol. 85, Advances in the Astronautical Sciences, Univelt, San Diego, 1993, pp. 1851–1870.

[7]Nixon, M. S., and Misra, A. K., "Nonlinear Dynamics and Chaos of Two Body Tethered Satellite Systems," *Astrodynamics 1993*, Vol. 85, Advances in the Astronautical Sciences, Univelt, San Diego, 1993, pp. 775–794.

[8]Fujii, A. H., and Ichiki, W., "Nonlinear Dynamics of the Tethered Subsatellite System in the Station Keeping Phase," *Journal of Guidance, Control, and Dynamics*, Vol. 20, No. 2, 1997, pp. 403–406.

[9]Socolar, J. E. S., Sukow, D. W., and Gauthier, D. J., "Stabilizing Unstable Periodic Orbits in Fast Dynamical Systems," *Physical Review E*, Vol. 50, No. 4, 1994, pp. 3245–3248.

[10]Bleich, M. E., and Socolar, J. E. S., "Stability of Periodic Orbits Controlled by Time-Delay Feedback," *Physics Letters A*, Vol. 210, Nos. 1–2, 1996, pp. 87–94.

[11]Fujii, A. H., Ichiki, W., Suda, S., and Watanabe, R. T., "Chaos Analysis on Librational Control of Gravity-Gradient Satellite in Elliptic Orbit," *Journal of Guidance, Control, and Dynamics*, Vol. 23, No. 1, 2000, pp. 145–147.

[12]Takeichi, N., Natori, M. C., and Okuizumi, N., "Libration Control of a Tethered System in Elliptic Orbits," *Journal of the Japan Society for Aeronautical and Space Science*, Vol. 49, No. 567, 2001, pp. 130–134 (in Japanese).

[13]Kane, T. R., and Levinson, D. A., *Dynamics: Theory and Applications*, McGraw–Hill, New York, 1985, Chap. 6.

[14]Wolf, A., Swift, J. B., Swinny, H. L., and Vastano, J. A., "Determining Lyapunov Exponents from a Time Series," *Physica 16D*, Elsevier, New York, 1985, pp. 285–317.